Environmental Science and Pollution Research (2023) 30:112503–112516
https://doi.org/10.1007/s11356-023-30290-5

RESEARCH ARTICLE

# Highly efficient removal of trace heavy metals by high surface area ordered dithiocarbamate-functionalized magnetic mesoporous silica

Najmedin Azizi[1] · Amin Rahimzadeh Oskooee[1] · Elham Farhadi[1] · Mostafa Saadat[1]

Received: 29 May 2023 / Accepted: 2 October 2023 / Published online: 13 October 2023


## Abstract

The study describes synthesizing and characterizing a novel dithiocarbamate-functionalized magnetic nanocomposite. This nanocomposite exhibits several desirable properties, including a large pore diameter of 2.55 nm, a high surface area of 1149 $m^2/g$, and excellent capturing capabilities. The synthesis process involves the preparation of highly porous magnetic nanocomposites, followed by functionalization with dithiocarbamate functional groups through a reaction with carbon disulfide and amine. The synthesized nanocomposite was thoroughly characterized using various techniques, including X-ray diffraction analysis, transmission electron microscopy, scanning electron microscopy, Fourier-transform infrared spectroscopy, and thermogravimetric analysis. The performance of the mesoporous nanocomposite as an adsorbent for removing Pb(II), Cd(II), and Cu(II) cations from contaminated water was evaluated. The study finds that the maximum removal efficiency for Pb(II), Cd(II), and Cu(II) cations is achieved at pH values above 4. The optimal contact time for achieving 100% removal efficiency of the mentioned cations ranged between 60 and 120 min. Within this time range, the adsorbent exhibited efficient capture of the heavy metal cations from contaminated water. Additionally, the appropriate amount of adsorbent required for complete elimination of the heavy metal cations is determined. For Cd(II), the optimal dosage was found to be 50 mg of the adsorbent. For Cu(II), the optimal dosage was determined to be 40 mg. Finally, for Pb(II), the optimal dosage was 30 mg. The adsorbent's regeneration capability was demonstrated, showing that it could be reused for five consecutive runs.

**Keywords** Porous nanocomposite · Dithiocarbamate functional groups · Contaminated water · Magnetic mesoporous silica

## Introduction

The contamination of freshwater by harmful metal cations from industrial sources is a well-recognized global problem that poses a significant threat to the lives of people residing in polluted regions (Salomons 1995). While certain heavy metals are essential in small quantities, elevated levels of these pollutants can have severe and detrimental effects on human and animal health (Siegel and Martin 1994; Madoni et al. 1996). Some essential industrial metals, including copper, cadmium, lead, and zinc, are common environmental pollutants. Copper plays a vital role in biological systems as a catalyst for iron absorption. However, excessive amounts of copper can lead to severe illnesses such as stomach and intestinal distress and liver and kidney damage (Johnson 1990). Cadmium and lead, on the other hand, are non-essential cations that can cause a host of biological and physical disorders, even in trace amounts (Johnson 1990; Waseem et al. 2011). Moreover, these cations have been found to contribute to kidney stone formation in the human body (Friberg et al. 1979; Lo et al. 1999; Goel et al. 2005).

Consequently, numerous studies and efforts have been conducted to remove these heavy metals from aquatic systems to ensure safe and clean drinking water. Various approaches have been explored, including the use of natural compounds or modified natural compounds. For example, creosote bush has been investigated for its potential in heavy metal removal (Gardea-Torresdey et al. 1998). Additionally, techniques utilizing *Penicillium digitatum* immobilized on pumice stone (Baytak and Türker 2009), zeolites pumice with calcined alunite (Catalfamo et al. 2006), zero-valent iron/pumice permeable reactive barriers (Moraci and Calabrò 2010), removal of uranium(VI)

Responsible Editor: Angeles Blanco

✉ Najmedin Azizi
azizi@ccerci.ac.ir

[1] Chemistry & Chemical Engineering Research Center of Iran, P.O. Box 14335-186, Tehran, Iran

ions from aqueous solutions using Schiff base functionalized SBA-15 mesoporous silica materials (Dolatyari et al. 2016) and hebba clay and activated carbon (Shama and Gad 2010) have shown promise in removing these contaminants from water sources. Furthermore, significant research has been conducted on the development of effective methodologies to eliminate metal cation contamination from polluted water. Synthetic substances, such as ion exchanger membranes (Ahmad et al., 2007), carbon nanotubes (Kosa et al. 2012), and functionalized silica gel and other silicate structures (Mahmoud 1999; Mahmoud et al. 2004), have been investigated for their potential in removing heavy metals from water sources. These endeavors aim to address the challenges posed by metal cation contamination and ensure the availability of clean and safe water resources for communities. Continued research and innovation in this field are crucial to developing efficient and sustainable metal cation removal techniques from contaminated water sources.

In addition to the mentioned approaches, mesoporous materials have been utilized as novel compounds for various applications, including heavy metal separation, owing to their advantageous properties, such as high surface area, large pore diameter, and low density. These materials have found applications in fields like catalysts (Goubert-Renaudin et al. 2009a; Shuklov et al. 2007) and heavy metal separation (Ho et al. 2002; Aguado et al. 2009; Oh et al. 2007; Fu and Huang 2018) due to their surfaces being modified with different functional groups (Biswas et al. 2021; Wang et al. 2020; Yaqoob et al. 2020; Al Hamouz and Estatie 2017; Hong et al. 2022; Ibrahim et al. 2022; Yu et al. 2022; Dong et al. 2022; Pournara et al. 2021).

Dithiocarbamate functional groups have shown great potential as efficient complexing agents for heavy metal removal when incorporated into various structures (Jing et al. 2009; Goubert-Renaudin et al. 2009b; Bai et al. 2011). Dithiocarbamate-based adsorbents operate on the principle of chelation or complexation, where the sulfur atoms in the dithiocarbamate functional groups form strong coordinate bonds with heavy metal cations, resulting in stable metal-dithiocarbamate complexes (Zhang et al, 2021) . This coordination interaction allows for efficient and selective adsorption of heavy metal ions (Zhang et al. 2020; Sari and Tuzen 2019; Huang et al. 2020). The choice of dithiocarbamate ligand, such as diethyldithiocarbamate, sodium diethyldithiocarbamate, and N,N-diethyl-N-benzyl dithiocarbamate, can influence the adsorption capacity, selectivity, and stability of the adsorbent (Wang et al. 2018). Dithiocarbamate-based adsorbents can be synthesized by incorporating dithiocarbamate functional groups onto various support materials, including activated carbon, silica gel, polymers, and magnetic nanoparticles (Raval and Shah 2019; Sari and Tuzen 2017). These adsorbents exhibit high affinity and selectivity towards a wide range of heavy metal cations, including lead (Pb), cadmium (Cd), copper (Cu), zinc (Zn), mercury (Hg), and nickel (Ni), effectively removing them from aqueous solutions, even at low concentrations (Zhang et al. 2019). The utilization of mesoporous materials combined with dithiocarbamate functional groups holds promise for the development of efficient and sustainable techniques for heavy metal separation and remediation (Girginova et al. 2010). However, further research is needed to enhance removal efficiency, increase surface area, optimize separation processes, (Li et al, 2020) and improve recovery conditions (Gardea-Torresdey et al. 1998).

To overcome these limitations, continued research should optimize the adsorbent design, enhance the surface area and adsorption capacity, and develop efficient separation and recovery processes. By addressing these challenges, it is possible to develop improved techniques for heavy metal removal that offer higher removal efficiencies, shorter separation times, and easier recovery processes. Such advancements would contribute to developing more effective and sustainable water treatment technologies for mitigating heavy metal contamination in natural waters.

In recent years, we have focused on developing novel dithiocarbamate chemistry (Azizi et al. 2014; Azizi et al. 2006) and exploring its application in magnetic nanoparticle systems (Yazdani et al. 2016; Seyyed Shahabi et al. 2019). In this study, we present the synthesis of a novel magnetic α-$Fe_2O_3$/MCM-41@Pr-DTC material, functionalized with dithiocarbamate groups. This material exhibits desirable properties such as a large pore diameter of 2.55 nm, a high surface area of 1149 $m^2$/g, and excellent adsorption capabilities for Cu, Cd, and Pb cations from contaminated water sources. To evaluate the performance of the adsorbent, we conducted experimental studies to determine the removal efficiency of Cu, Cd, and Pb divalent cations. Optimum pH and time were determined, and the number of adsorbents required to achieve maximom removal efficiency was identified.

## Experimental

### Chemical

$FeCl_3{\cdot}6H_2O$, $FeCl_2{\cdot}4H_2O$, cetyltrimethylammonium bromide (CTAB), tetraethyl orthosilicate (TEOS), 3-aminopropyltrimethoxysilane (APTES), 2-propanol, toluene, NaOH, carbon disulfide, $Cd(NO_3)_2.5H_2O$, $Pb(NO_3).5H_2O$, $CuSO_4.5H_2O$, and $HNO_3$ are analytical grade and were purchased from Merck.

### Instruments

The synthesized mesoporous silica material was characterized using various analytical techniques. The details of the instruments used for each analysis are as follows:

1. Fourier-transform infrared spectroscopy (FTIR): The KBr disk method was employed for FTIR analysis, and the measurements were conducted using a Shimadzu IR-460 model spectrometer.
2. $N_2$ adsorption-desorption: The surface area, pore size distribution, and pore volume of the synthesized silica were determined by $N_2$ adsorption-desorption analysis. The measurements were performed using a desorb (mini II model) instrument based on the Brunauer-Emmett-Teller (BET) and Barrett-Joyner-Halenda (BJH) methods.
3. X-ray diffraction (XRD): The crystalline structure of the synthesized material was examined using XRD analysis. XRD patterns were measured using a Philips Analytical instrument with a Co anode.
4. Thermal gravity analysis (TGA): The thermal stability and decomposition behavior of the synthesized silica were analyzed using TGA. TGA measurements were carried out using a NETZSCH (Iris 20g 2-7 model) instrument.
5. Scanning electron microscopy (SEM): The surface morphology and microstructure of the synthesized material were visualized using scanning electron microscopy. SEM images were captured using a TESCAN Vega model instrument. TEM images were obtained using a Zeiss EM900 instrument.

## Preparation of α-$Fe_2O_3$/MCM-41@Pr-DTC

The preparation of magnetic α-$Fe_2O_3$/MCM-41@Pr-DTC was carried out in three steps, following the literature mentioned.

### Preparation of magnetic $Fe_2O_3$/MCM-41

The synthesis of magnetic $Fe_2O_3$/MCM-41 to support functionalization with the dithiocarbamate functional group was performed according to Chen et al. (Chen et al. 2009). The synthesis involves a stepped approach, starting with the preparation of magnetic iron oxide ($Fe_3O_4$) nanoparticles, followed by their insertion into the mesoporous silica structure. In the first step, 3 g of $FeCl_3$ and 1.2 g of $FeCl_2$ were dissolved in 20 mL of deionized water degassed with $N_2$ flow. Then, a 100 mL solution of $NH_3.H_2O$ (1 M) containing 0.4 g of CTAB surfactant was added under an ultrasonic probe. The resulting mixture was sonicated for 60 min, and the colloidal $Fe_3O_4$ nanoparticles were separated using an external 1.2 Tesla magnet. Next, for the synthesis of $Fe_3O_4$/MCM-41 mesoporous silica, the as-synthesized $Fe_3O_4$ nanoparticles were added to a 2 L solution containing 1280 mL of degassed deionized water, 720 mL of ammonia solution (15 M), and 11.6 g of CTAB under constant mechanical stirring in a nitrogen environment. After 30 min, 46.4 mL of TEOS was added dropwise to the above solution, and stirring was continued at 30 °C for 24 h. The resulting $Fe_3O_4$/MCM-41 nanocomposite was collected with an external 1.2 T magnet. A surfactant removal process was also conducted to convert the $Fe_3O_4$ nanoparticles to high surface area $Fe_2O_3$ magnetic nanoparticles. This removal process involved calcination at 450 °C for 4 h, following the method outlined in the reference by Mishra et al. (2019).

### Functionalization of $Fe_2O_3$/MCM-41 with the propylamine group

According to the reported procedure by McKittrick and Jones (2003), 5 g of $Fe_2O_3$/MCM-41 mesoporous silica was typically dried at 150 °C in a vacuum oven for 12 h and then suspended in 250 mL of dried toluene. Subsequently, 7 mL of 3-aminopropyltriethoxysilane (APTES) was added dropwise to the suspension, which was then mechanically stirred and refluxed for 24 h. After magnetic collection, the suspension was purified using Soxhlet extraction with toluene for 24 h to remove any organic impurities, particularly APTES. The resulting powder was subsequently dried in a vacuum oven and subjected to characterization.

### Preparation of α-$Fe_2O_3$/MCM-41@Pr-DTC

According to the reported methods, (Pournara et al. 2021), 630 mg of $Fe_2O_3$/MCM-41@Pr-$NH_2$ was added to the reaction medium, which consisted of 200 mL of 1 M NaOH, 400 mL of isopropanol, and 30 mL of $CS_2$, in an ice bath. The mixture was stirred at room temperature for 6 h. The magnetic nanocomposite was then separated using an external magnet, washed with isopropanol, and dried under a vacuum.

### Heavy metal cations (Cu(II), Cd(II) and Pb(II)) adsorption studies

A 20 mL of 50 mg/L standard solution of Cu(II), Cd(II), and Pb(II) cations was prepared to optimize the adsorption parameters. To prepare 50 mg/L standard solutions of the selected cations, stock solutions of $Cd(NO_3)_2{\cdot}5H_2O$, $Pb(NO_3)_2{\cdot}5H_2O$, and $CuSO_4{\cdot}5H_2O$ with concentrations of 250 mg/L were diluted in water. The pH of the solutions was adjusted from 2 to 6 using standard solutions of $HNO_3$. The effects of pH, contact time, and the amount of adsorbent in the 50 mg/L standard solution were investigated. Additionally, to compare the effectiveness of the dithiocarbamate functional group in capturing heavy metal cations, $Fe_2O_3$/MCM-41@Pr-$NH_2$ was experimentally employed to remove the targeted heavy metals from standard solutions under similar conditions of pH, time, and the amount of adsorbent. Furthermore, the regeneration

of the adsorbent was studied to evaluate its reusability. The removal efficiency of $Fe_2O_3$/MCM-41@Pr-DTC was calculated using the formula $\%R = (C_0 - C_e) / C_0$, where $C_0$ represents the initial concentration of the heavy metal cation, and $C_e$ denotes the concentration of the heavy metal cations at the sampling time after removal using $Fe_2O_3$/MCM-41@Pr-DTC.

### Study the effect of pH parameter with $Fe_2O_3$/MCM-41@Pr-DTC adsorbent

To determine the optimum pH for the removal of heavy metal cations in the presence of $Fe_2O_3$/MCM-41@Pr-DTC adsorbent, 20 mL of the stock solution of heavy metal cations at concentrations of 50 mg/L, ranging from pH 2 to pH 6 (Cu(II), Cd(II), and Pb(II)), were transferred to individual test tubes. Each test tube contained 20 mg of α-$Fe_2O_3$/MCM-41@Pr-DTC adsorbent. The mixtures were shaken for 120 min, after which the adsorbent was collected magnetically (Fig. 1). The concentrations of the heavy metal cations were determined using AAS (atomic absorption spectroscopy) technique. The removal efficiencies were calculated using the formula mentioned in Section "Heavy metal cations (Cu(II), Cd(II) and Pb(II)) adsorption studies." A similar process was carried out using $Fe_2O_3$/MCM-41@Pr-$NH_2$ adsorbent instead of $Fe_2O_3$/MCM-41@Pr-DTC adsorbent. The results of this part are presented in Fig. 11.

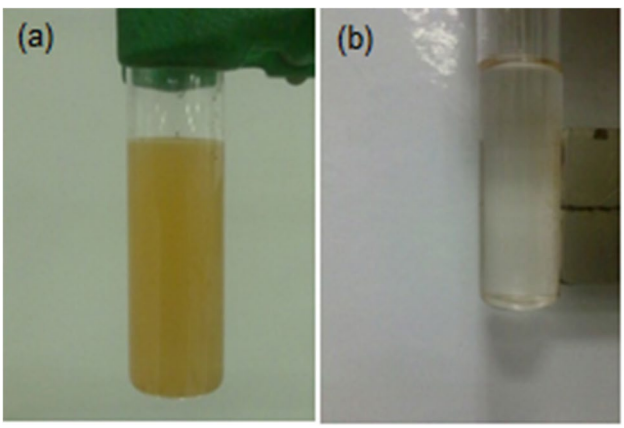


**Fig. 1** **a** Suspension of MCM-41-DTC adsorbent in heavy metal solution after the adsorption process and (**b**) in the presence of external magnetic field

### Study the effect of contact time

In this section, the adequate contact time between a 50 mg/L solution of Cu, Cd, and Pb divalent cations and $Fe_2O_3$/MCM-41@Pr-DTC adsorbent was investigated. The concentration of each cation solution was measured at the optimum pH (determined from the data extracted in Fig. 11). A 20 mL solution containing 20 mg of $Fe_2O_3$/MCM-41@Pr-DTC adsorbent was prepared for each cation solution, and the contact time was varied at intervals of 10, 30, 60, 90, and 120 min. The results are presented in Fig. 15. To conduct the experiment, 20 mg of $Fe_2O_3$/MCM-41@Pr-DTC adsorbent was added to a test tube containing 20 mL of the 50 mg/L solution for each heavy metal cation. The mixture was then shaken for the specified durations. Afterward, the solution was diluted 10 times, and the cation concentration was determined using the AAS method. The removal efficiencies were calculated using the formula mentioned in Section "Heavy metal cations (Cu(II), Cd(II) and Pb(II)) adsorption studies," and the results were plotted in Fig. 15.

### Study the effect of the amount of adsorbent

To optimize the amount of $Fe_2O_3$/MCM-41@Pr-DTC adsorbent for removing Cu(II), Cd(II) and Pb(II) cations from standard solutions, different amounts of adsorbent according to Table 1 were added to 20 mL of 50 mg/L of mentioned cations in separated tubes for every cation solution; the optimized time and pH and the concentration of elements were measured via AAS method after magnetic separation of $Fe_2O_3$/MCM-41@Pr-DTC adsorbent from medium, and removal efficiency was calculated by formula mentioned in Section "Heavy metal cations (Cu(II), Cd(II) and Pb(II)) adsorption studies" (Fig. 16).

## Regeneration of $Fe_2O_3$/MCM-41@Pr-DTC adsorbent

To investigate the reusability of $Fe_2O_3$/MCM-41@Pr-DTC, the adsorbent was regenerated using a 0.1 M aqueous solution of HCl. After magnetic separation of the adsorbent from the adsorption system, the used $Fe_2O_3$/MCM-41@Pr-DTC adsorbent was transferred to a tube. Then, 5 mL of the 0.1 M HCl solution was added, and the mixture was shaken using a shaker for 2 h. The adsorbent

**Table 1** The amount of α-$Fe_2O_3$/MCM-41@Pr-DTC adsorbent in removing of Cu(II), Cd(II), and Pb(II) cations from standard aqueous solutions in optimized pH and time

| Type of cation | Cu(II) Cd(II) Pb(II) | Cu(II) Cd(II) Pb(II) | Cu(II) Cd(II) Pb(II) | Cu(II) Cd(II) Pb(II) | Cu(II) Cd(II) Pb(II) | Cu(II) Cd(II) Pb(II) |
|---|---|---|---|---|---|---|
| Adsorbent amount(mg) | 5 | 8 | 11 | 14 | 17 | 20 |

was subsequently collected magnetically, dried in a vacuum oven, and reused in subsequent runs. The regeneration process was repeated for a total of 4 runs. In each run, 20 mg of $Fe_2O_3$/MCM-41@Pr-DTC adsorbent was used in 20 mL of a 50 mg/L solution of each respective cation, as described in Section "Study the effect of pH parameter with $Fe_2O_3$/MCM-41@Pr-DTC adsorbent." After each run, the removal efficiency of the adsorbent was calculated using the mentioned formula. The results of the reusability study are presented in Fig. 17, illustrating the removal efficiency after each consumption of the $Fe_2O_3$/MCM-41@Pr-DTC adsorbent.

## Result and discussion

### Characterization of $Fe_2O_3$/MCM-41

The SEM images of $Fe_2O_3$/MCM-41 at different zoom levels show irregular morphologies, with the dominant structures being prism and round shapes (Fig. 2 and supporting information). This indicates the presence of various morphological features in the mesoporous silica.

Furthermore, the TEM image of the synthesized $Fe_2O_3$/MCM-41 mesoporous silica (Fig. 3 and supporting information) reveals regular and smooth pores within the structure. The image also shows clusters of $Fe_2O_3$ nanoparticles embedded in the mesoporous system. This confirms the successful incorporation of $Fe_2O_3$ nanoparticles within the $Fe_2O_3$/MCM-41 mesoporous silica.

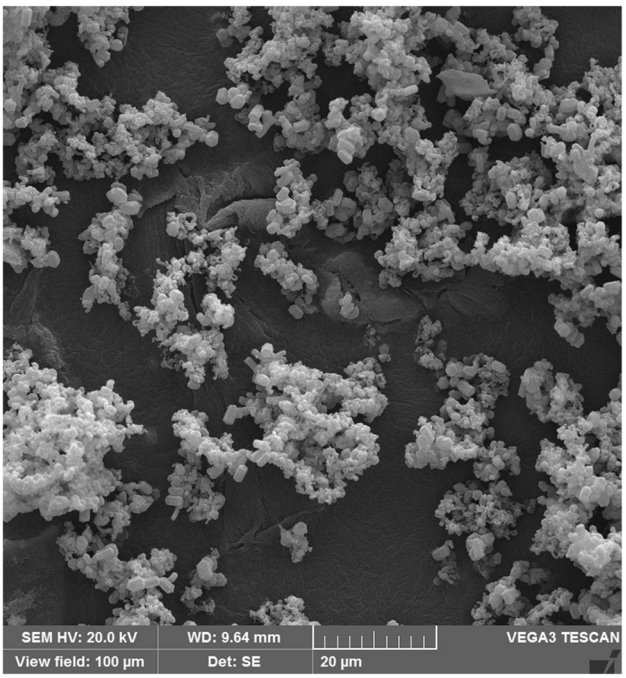


**Fig. 2** SEM images of $Fe_2O_3$/MCM-41 mesoporous silica

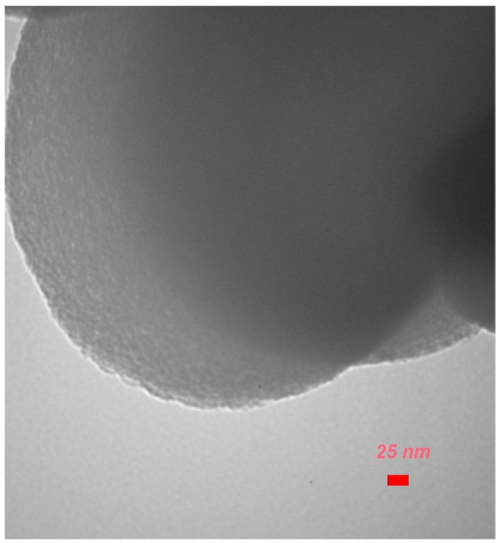


**Fig. 3** TEM Image of $Fe_2O_3$/MCM-41 mesoporous silica

### Characterization of $Fe_2O_3$/MCM-41@Pr-DTC

#### XRD analysis

In the low-angle XRD spectra (Fig. 4), the peak observed at 2.63° with reduced intensity indicates that the pore structure of the $Fe_2O_3$/MCM-41@Pr-DTC mesoporous silica has changed as a result of the functionalization with the dithiocarbamate functional group. This suggests alterations in the mesoporous structure due to the functionalization process. In the wide-angle X-ray diffraction pattern (Fig. 5), the presence of peaks at angles 30.5°, 35.6°, 43.4°, 57.2°, and 62.9° confirms the existence of the

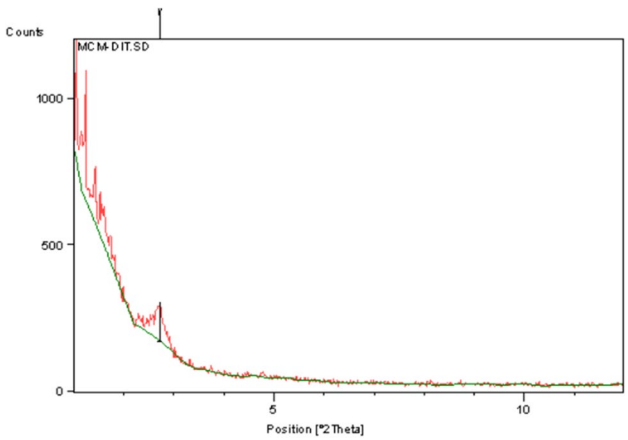


**Fig. 4** Small-angle XRD pattern of $Fe_2O_3$/MCM-41@Pr-DTC

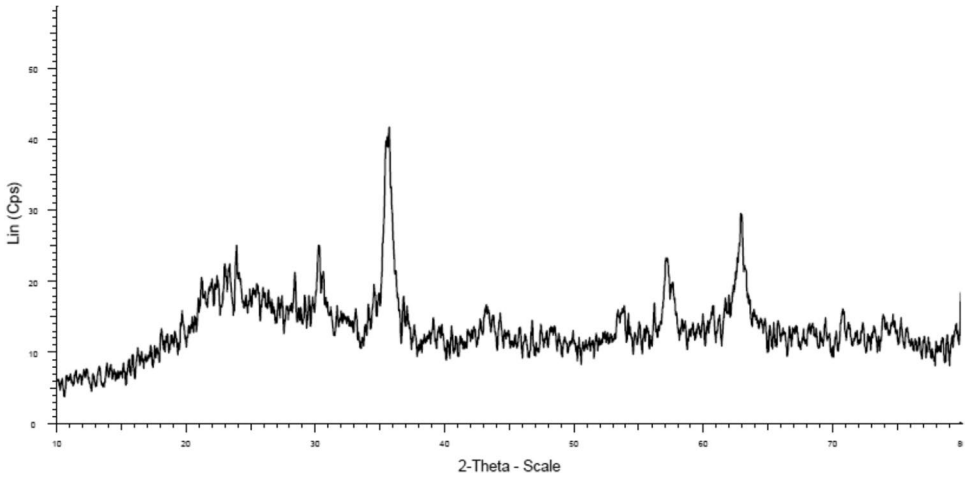


**Fig. 5** The wide-angle XRD pattern of $Fe_2O_3$/MCM-41@Pr-DTC

magnetite cubic spinel structure of $Fe_2O_3$ nanoparticles in the mesoporous silica. These peaks indicate the stability of the $Fe_2O_3$ nanoparticles during the synthesis and functionalization processes. Furthermore, the presence of cluster groups suggests that the $Fe_2O_3$ nanoparticles are present in aggregated forms within the functionalized mesoporous silica.

### $N_2$ adsorption-desorption isotherms

The $N_2$ adsorption-desorption isotherms of $Fe_2O_3$/MCM-41@Pr-DTC are presented in Fig. 6a, Fig. 6b, Fig. 6c. These isotherms provide information about the adsorption and desorption of nitrogen gas on the material. According to the results of the analysis presented in Table 2, the surface area of $Fe_2O_3$/MCM-41@Pr-DTC is determined to be 1149 $m^2$/g. This surface area is reduced compared to $Fe_2O_3$/MCM-41 mesoporous silica. The presence of the dithiocarbamate functional group in $Fe_2O_3$/MCM-41@Pr-DTC is responsible for this reduction in surface area. The pore size of $Fe_2O_3$/MCM-41@Pr-DTC is measured to be 2.51 nm, indicating a decrease in pore diameter compared to $Fe_2O_3$/MCM-41. This decrease in pore diameter (0.37 nm) suggests the incorporation of the bulk propyl dithiocarbamate functional groups within the Fe2O3/MCM-41 mesoporous silica structure. Additionally, the mean pore volume of $Fe_2O_3$/MCM-41@Pr-DTC is determined to be 0.723 $cm^3$/g, which is lower than that of $Fe_2O_3$/MCM-41. The subtraction observed in the pore volume indicates a decrease in available pore space, further confirming the presence of bulk propyl dithiocarbamate functional groups within the structure of $Fe_2O_3$/MCM-41 mesoporous silica.

### Microscopic study on the $Fe_2O_3$/MCM-41@Pr-DTC

The SEM image of $Fe_2O_3$/MCM-41@Pr-DTC mesoporous silica in Fig. 7 and supporting information shows a dominant hexagonal prism structure. This suggests that the hexagonal prism morphology is prevalent in the $Fe_2O_3$/MCM-41@Pr-DTC structure. Additionally, the observation that the structure of silica remains stable during the functionalization process with the dithiocarbamate group indicates that the functionalization does not significantly alter the overall morphology of the mesoporous silica.

The TEM image of $Fe_2O_3$/MCM-41@Pr-DTC mesoporous silica is presented in Fig. 8 and the supporting information. It appears that the structure of the material exhibits uniform and equal-sized pores. This suggests that the pore structure remains unchanged during the functionalization process with the dithiocarbamate group. Additionally, the presence of dark spot-shaped clusters of $Fe_2O_3$ within the construction of $Fe_2O_3$/MCM-41@Pr-DTC mesoporous silica indicates the existence of $Fe_2O_3$ aggregates or nanoparticles.

### Thermal gravity analysis of $Fe_2O_3$/MCM-41@Pr-DTC

The thermal gravity analysis demonstrates the mass changes of the composite as a function of temperature (Fig. 9). The analysis of the $Fe_2O_3$/MCM-41@Pr-DTC reveals a mass loss observed up to 190 °C. This mass loss is attributed to the decomposition of the dithiocarbamate functional group and water absorbed from the environments present in the $Fe_2O_3$/MCM-41@Pr-DTC structure. The decomposition of the dithiocarbamate functional group results in the formation of amine and carbon disulfide due to the high temperature. Following the initial mass loss, there is a subsequent mass change observed from 190 to 300 °C. This mass change is associated with the loss of the propylamine group attached to the mesoporous silica structure of $Fe_2O_3$/MCM-41@Pr-DTC.

The FTIR spectrum of $Fe_2O_3$/MCM-41@Pr-DTC mesoporous silica is shown in Fig. 10. The peak observed at the wavenumber of 588 $cm^{-1}$ corresponds to the

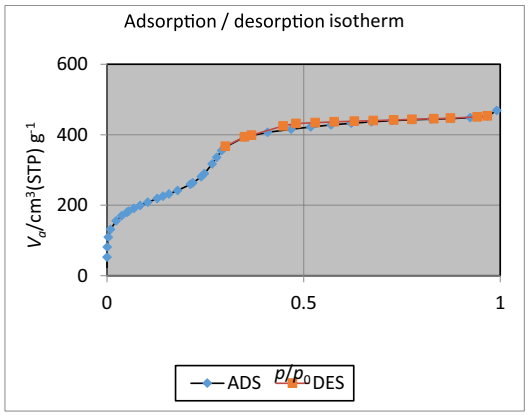


a)

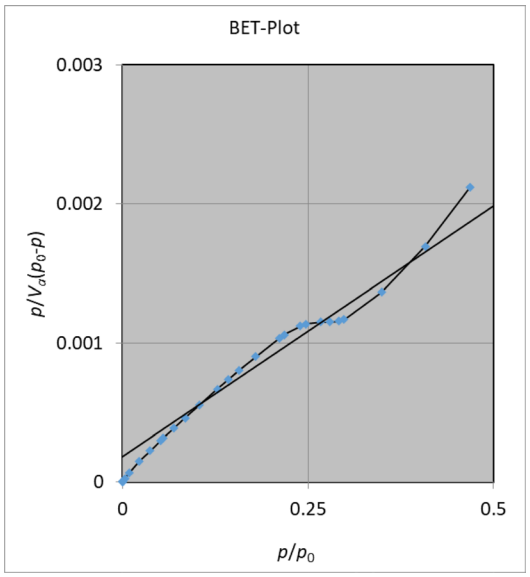


b)

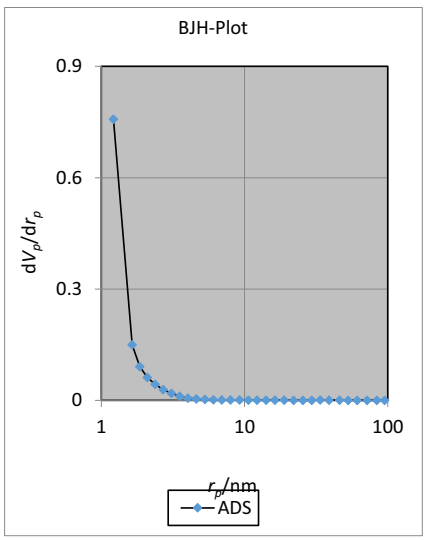


c)

**Fig. 6** **a** $N_2$ adsorption-desorption isotherm, **b** BET, and **c** BJH plot of $Fe_2O_3$/MCM-41@Pr-DTC

**Table 2** BET surface area, pore volume, and average pore diameter values of $Fe_2O_3$/MCM-41@Pr-DTC

| Mesoporous silica | BET surface area | Pore volume | Average pore diameter |
|---|---|---|---|
| $Fe_2O_3$/MCM41@ Pr-DTC | 1149 $m^2$/g | 0.723 [$cm^3$/g] | 2.51 nm |

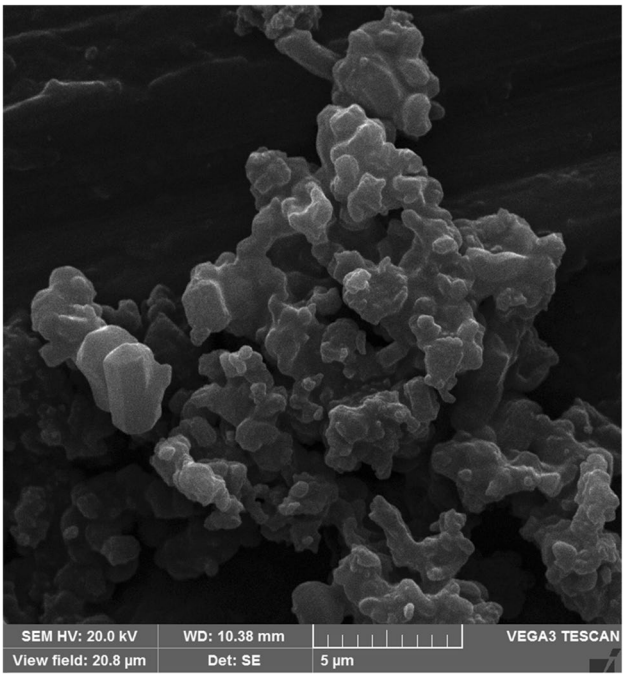


**Fig. 7** SEM image for $Fe_2O_3$/MCM-41@Pr-DTC

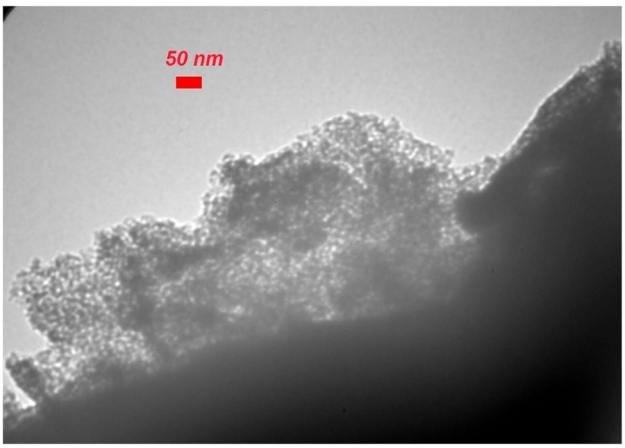


**Fig. 8** TEM image of $Fe_2O_3$/MCM-41@Pr-DTC

stretching vibrations of Fe-O bonds. This peak indicates the presence of $Fe_2O_3$ nanoparticles attached to the silica surface. The peak appearing at 1633 $cm^{-1}$ is associated

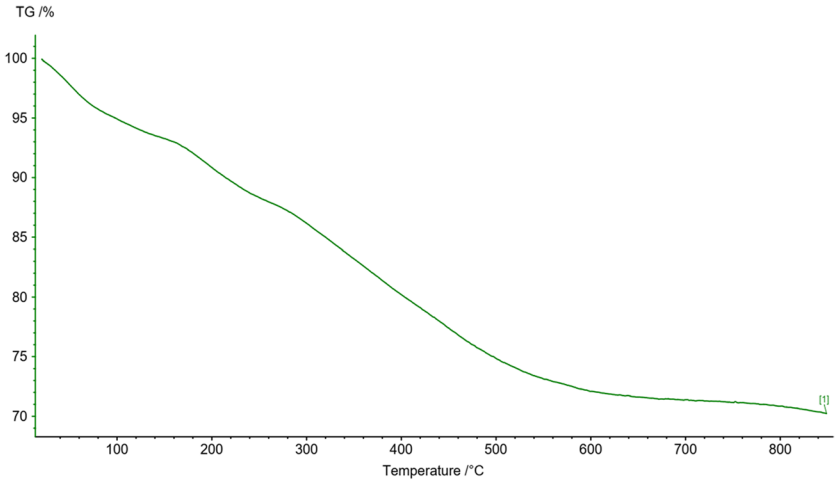


**Fig. 9** Thermal gravity analysis of $Fe_2O_3$/MCM-41@Pr-DTC

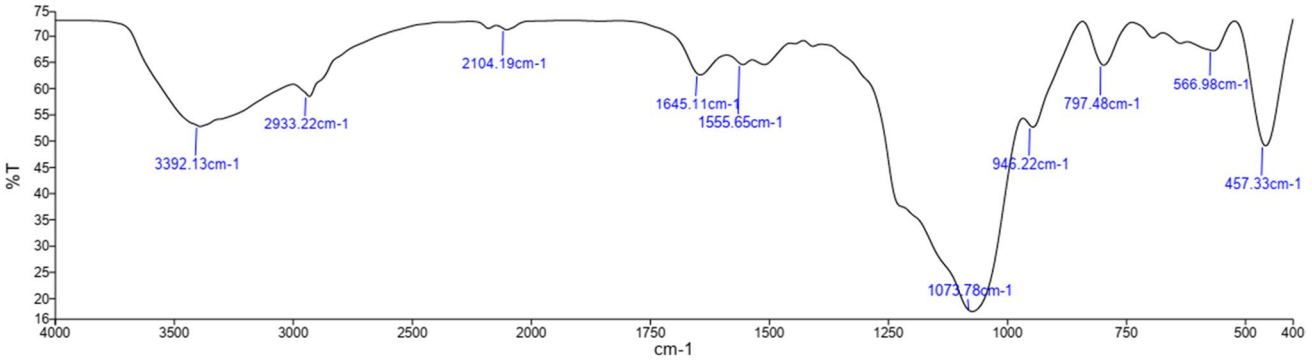


**Fig. 10** FTIR spectra of $Fe_2O_3$/MCM-41@Pr-DTC

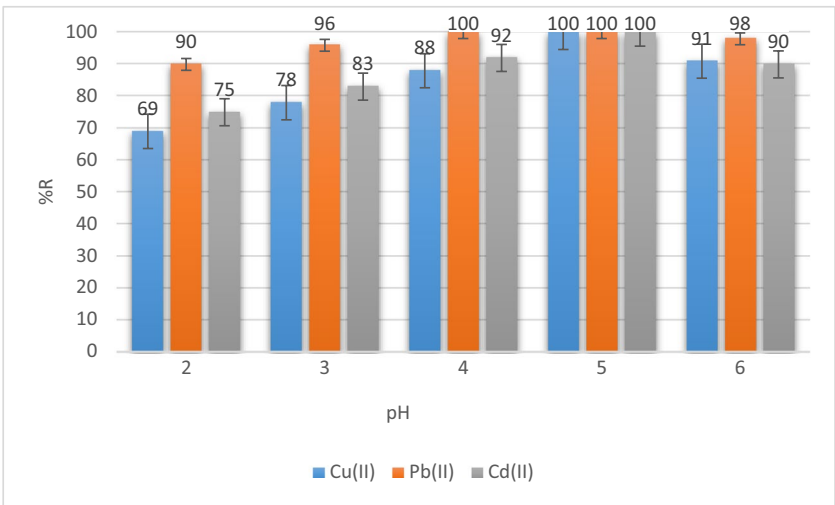


**Fig. 11** The removal efficiency of Cu, Pb, and Cd cation solutions from standard 50 mg/L solutions of these cations in the presence of $Fe_2O_3$/MCM-41@Pr-DTC adsorbent

with the bending vibrations of water molecules adsorbed on the silica surface and dithiocarbamate groups. Three peaks observed at wavenumbers $436^{-1}$, $804^{-1}$, and $1077^{-1}$ are related to Si-O-Si bonds. The broad peak in the 3000–3500 $cm^{-1}$ range corresponds to water absorbed from the environment and hydrogen bonding related to the

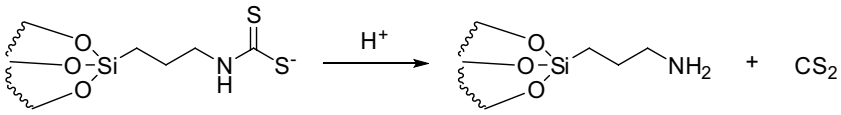


**Fig. 12** The decomposition of dithiocarbamate functional group to amine and carbon disulfide

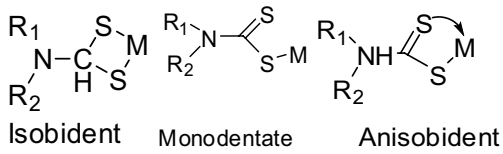


**Fig. 13** Different mechanisms of capturing heavy metal cations via dithiocarbamate functional groups

surface Si-OH groups of the magnetic mesoporous silica MCM-41.

## Optimization of various parameters on the removal efficiency of heavy metals in the presence of $Fe_2O_3$/MCM-41@Pr-DTC adsorbent

This study aimed to evaluate the impact of pH, contact time, and the amount of $Fe_2O_3$/MCM-41@Pr-DTC adsorbent on the efficiency of heavy metal ion removal. We sought to understand the chemical reasons or mechanisms underlying the observed removal efficiency values.

### Study the effect of pH

In standard conditions, different removal efficiency values were obtained for the mentioned heavy metal divalent cations. These parameters include pH, contact time, the initial concentration of heavy metal ions, and adsorbent dosage. The varying removal efficiency values suggested that different factors or conditions can influence the adsorption performance of each heavy metal cation. These factors include the chemical nature of the heavy metal cation, its interaction with the adsorbent surface, the presence of competing ions in the solution, and potential limitations or characteristics of the adsorbent material itself. To further understand the reasons behind the different removal efficiency values, it would be necessary to analyze the specific experimental conditions, including the importance of parameters such as pH, contact time, and adsorbent dosage and their interactions with the characteristics of the heavy metal cations and the adsorbent material. Additionally, considering the specific adsorption mechanisms involved and any potential limitations of the adsorbent would contribute to a comprehensive understanding of the observed variations in removal efficiency.

The maximum removal efficiency for Pb(II), Cd(II), and Cu(II) cations occurs at pH values above 4 (Fig. 11). This trend can be attributed to the decomposition of dithiocarbamate functional groups to silica-crafted amine groups and carbon disulfide under high concentrations of nitric acid (Fig. 12). The transition from dithiocarbamate to amine groups reduces the adsorption capacity for heavy metal cations (Fig. 13). Additionally, when comparing the capturing ability of dithiocarbamate functional groups to amine groups in capturing heavy metal cations from a standard solution, it was found that the removal efficiencies of the considered heavy metals decreased when using amine groups (Fig. 14). This decrease in removal

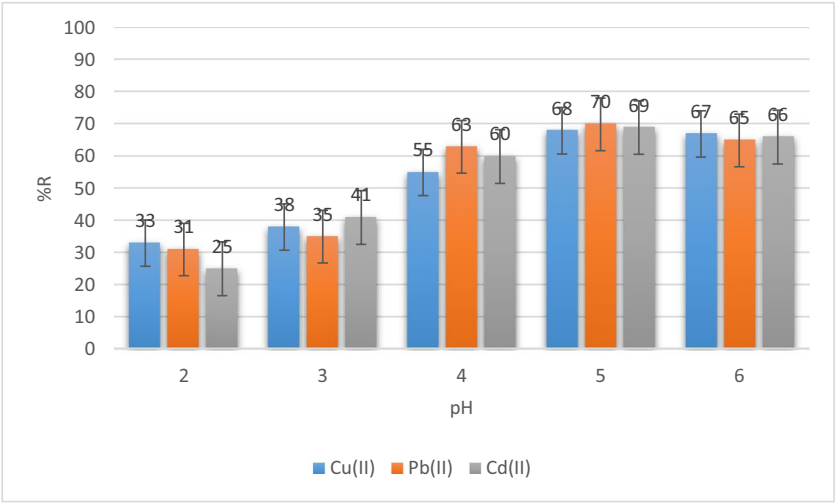


**Fig. 14** Removal efficiency of amine functionalized $Fe_2O_3$/MCM-41 mesoporous silica in the elimination of heavy metal cations

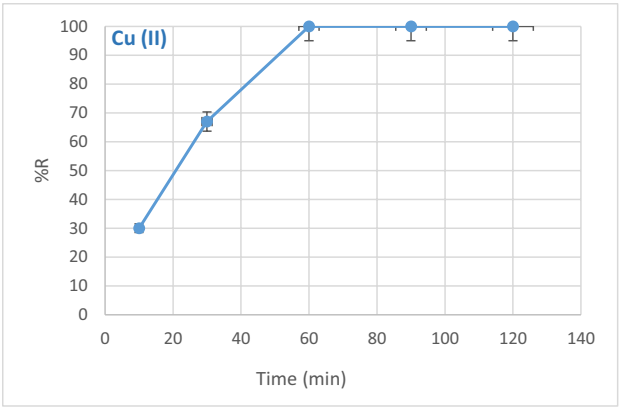


a)

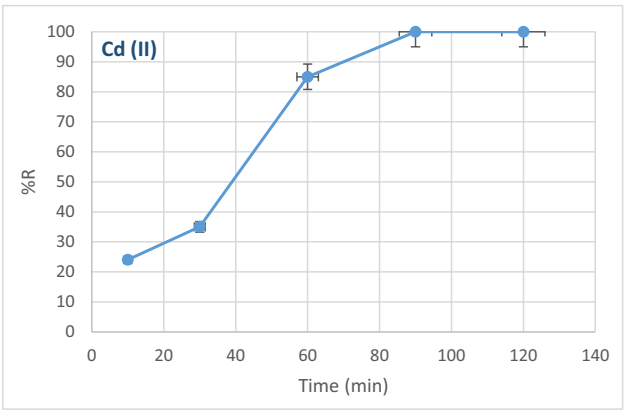


b)

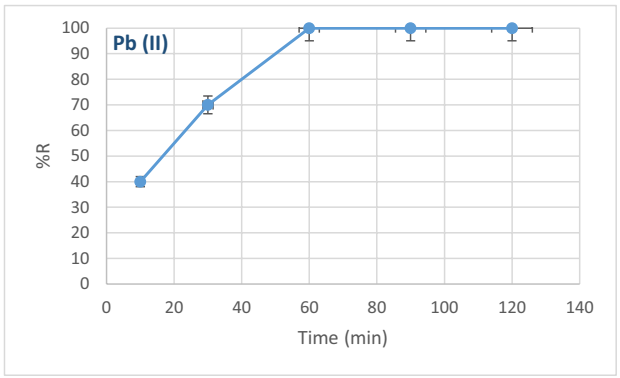


c)

**Fig. 15** Effect of time for removal of 50 mg/L **a** Cu(II), **b** Cd(II), and **c** Pb(II) cations via $Fe_2O_3$/MCM-41@Pr-DTC adsorbent

efficiency could be associated with the practical capturing ability of amines and dithiocarbamate functional groups, which operate through various mechanisms (Fig. 13).

### Study the effect of time

The impact of contact time on the efficiency of $Fe_2O_3$/MCM-41@Pr-DTC adsorbent in treating a 50 mg/L solution of Cd(II), Cu(II), and Pb(II) cations is depicted in Fig. 15. The graph demonstrates the optimal contact time required for achieving 100% removal efficiency of the mentioned cations. Notably, the time range between 60 and 120 min exhibits significant surface adsorption kinetics of $Fe_2O_3$/MCM-41@Pr-DTC mesoporous silica as an adsorbent in eliminating Cd(II), Cu(II), and Pb(II) cations from contaminated water. This suggests the presence of different mechanisms involved in capturing heavy metal cations using the dithiocarbamate functional group (as shown in Fig. 12) within a short duration.

### Study the effect of the amount of $Fe_2O_3$/MCM-41@Pr-DTC

Figure 16 illustrates the amount of $Fe_2O_3$/MCM-41@Pr-DTC adsorbent required in 20 mL solutions containing 50 mg/L of the mentioned cations. Based on the findings in Sections "Study the effect of pH" and "Study the effect of time" of this study, it was determined that the maximum amount of $Fe_2O_3$/MCM-41@Pr-DTC mesoporous silica adsorbent needed for complete elimination (100%) of Cd(II) and Pb(II) cations in optimized pH conditions is 0.014 g in a 20 mL solution with a concentration of 50 mg/L. Similarly, for Cu(II) cations under similar conditions, the required amount of adsorbent is 0.017 g.

## The study of reusability of $Fe_2O_3$/MCM-41@Pr-DTC mesoporous silica adsorbent

According to the experimental section, the $Fe_2O_3$/MCM-41@Pr-DTC adsorbent was recovered using an acidic solution and reused. However, as illustrated in Fig. 17, the removal efficiency decreased over time. This decline in efficiency can be attributed to the decomposition of some dithiocarbamate functional groups on the surface of silica when exposed to acid, as depicted in Fig. 12. Naturally, this decomposition reduces the number of dithiocarbamate groups available on the surface, resulting in a decrease in adsorption capacity. Therefore, repeated use of the adsorbent in the presence of acid can lead to a reduction of its overall effectiveness in removing heavy metal cations.

The comparison between dithiocarbamate-based absorbents and other absorbents should be based on specific experimental conditions, target heavy metal ions, and desired removal efficiencies, as tabulated in Table 3. Reported absorbents have their own advantages and limitations depending on the specific application requirements. When comparing heavy metal ion removal using dithiocarbamate-based absorbents with other types of adsorbents, several factors come into play:

1. Selectivity: Dithiocarbamate-based absorbents, such as $Fe_2O_3$/MCM-41@Pr-DTC mentioned earlier, often exhibit high selectivity towards heavy metal ions. The dithiocarbamate functional group has a strong affinity for metal cations, allowing for efficient and specific

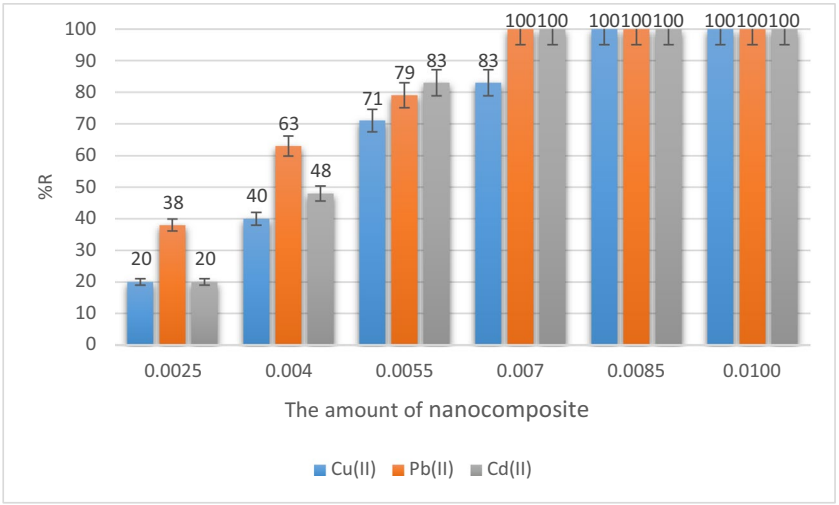


**Fig. 16** The different amounts of used $Fe_2O_3$/MCM-41@Pr-DTC

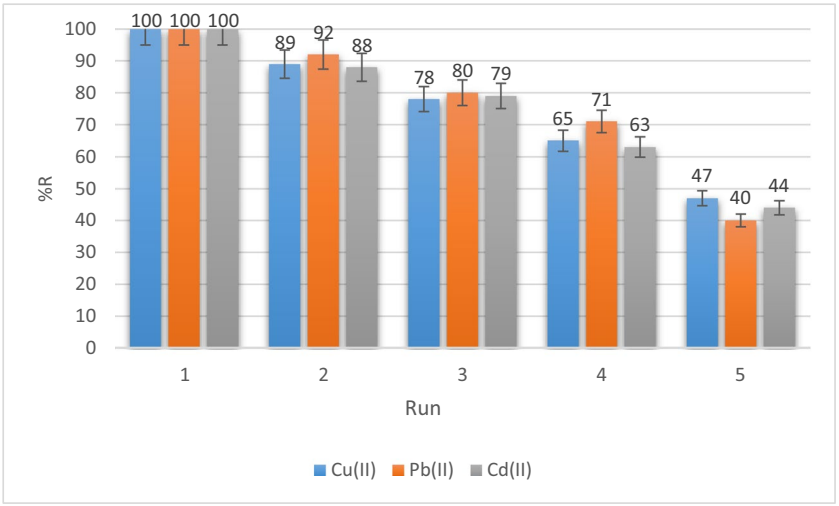


**Fig. 17** The reusability of $Fe_2O_3$/MCM-41@Pr-DTC mesoporous silica adsorbent after 5 runs of heavy metal cations adsorption and recycling by $HNO_3$ solution

**Table 3** Comparison between dithiocarbamate-based absorbents and other absorbent heavy metal ion removal

| Entry | Absorbent | Recyclability | Removal capacity (mg/g) | References |
|---|---|---|---|---|
| 1 | Carboxylated cellulose | 5 cycle | 82 | Tang et al. 2020 |
| 2 | Functionalized cryogels | 1 cycle | 108 | Kim and Lee 2019 |
| 3 | Barley Straw | 1 cycle | 4.6 | Pehlivan et al. 2012 |
| 4 | Chemically modified orange peel | 1 cycle | 289 | Feng et al. 2009 |
| 5 | Mango Peel | 1 cycle | 120 | Iqbal et al. 2009 |
| 6 | Sulfonated polyethersulfone | continues | 129 | Ibrahim et al. 2022 |
| 7 | Modified Fe/Co metal- | 1 cycle | 20 | Hong et al. 2022 |
| 8 | Melamine–formaldehyde | 1 cycle | 29 | Baraka et al. 2007 |
| 9 | Dithiocarbamate-modified cellulose | 1 cycle | 140 | Nakakubo et al. 2019 |
| 10 | $Fe_2O_3$/MCM-41@Pr-DTC | 5 cycle | 190 | This work |

removal. Other absorbents may have varying degrees of selectivity depending on their chemical composition and surface properties.

2. Adsorption capacity: The adsorption capacity of an absorbent determines how much of the target heavy metal ions it can capture. Dithiocarbamate-based absor-

bents generally have good adsorption capacities due to their specific binding interactions with metal cations. However, the adsorption capacity can also depend on the specific structure, surface area, and pore size of other absorbents.

3. Reusability: Reusability is an important aspect to consider for practical applications. Dithiocarbamate-based absorbents can often be regenerated and reused after desorption of the captured heavy metal ions. This is beneficial in terms of cost-effectiveness and sustainability. Other absorbents may or may not offer similar reusability, depending on their stability and regeneration methods.
4. Cost-effectiveness: The cost of synthesizing or obtaining the absorbent is a crucial factor in large-scale implementation. Dithiocarbamate-based absorbents can be synthesized using relatively inexpensive materials, making them cost-effective options. Other absorbents may vary in terms of production costs, availability, and scalability (Kim and Lee 2019) .

## Conclusion

This paper presents a comprehensive study on the development and utilization of a reusable $Fe_2O_3$/MCM-41@Pr-DTC adsorbent with several advantageous properties, including cost-effectiveness, stability, large pore diameter, and high surface area, for the efficient removal of heavy metal cations from contaminated water sources. The influence of pH, contact time, and adsorbent dosage on the efficiency of heavy metal ion removal using the $Fe_2O_3$/MCM-41@Pr-DTC adsorbent was tested. The findings provide valuable insights into optimizing the adsorption process for Cd(II), Cu(II), and Pb(II) cations. The study determined that a pH above 4 is favorable for achieving higher removal efficiency. Additionally, an optimal contact time ranging between 60 and 120 min was identified for achieving 100% removal efficiency. The results also revealed the appropriate adsorbent dosages: 50 mg for Cd(II), 40 mg for Cu(II), and 30 mg for Pb(II), under the specific experimental conditions studied. Furthermore, the study addressed the reusability of the adsorbent and observed a decline in removal efficiency over time due to the decomposition of dithiocarbamate functional groups when exposed to acid. The study emphasizes the need for a case-by-case evaluation when comparing different absorbents, taking into account factors such as selectivity, adsorption capacity, reusability, and cost-effectiveness. Furthermore, the reusability of the adsorbent is demonstrated through multiple cycles of acid washing, with only a decrease in adsorption efficiency observed after four consecutive runs.

**Supplementary Information** The online version contains supplementary material available at https://doi.org/10.1007/s11356-023-30290-5.

**Acknowledgements** This work is based upon research funded by Iran National Science Foundation (INSF) under project No.4013509.

**Author contribution** NA was involved in supervision, conception, and design. ARO performed material preparation and data collection, while MS conducted the analysis. The first draft of the manuscript was written by EF. All authors have read and approved the final manuscript.

**Data Availability** The data that support the findings of this study are available on request from the corresponding author.

## Declarations

**Ethics approval** Not applicable

**Consent to participate** Not applicable

**Consent to publish** Not applicable

**Competing interests** The authors declare no competing interests.

## References

Aguado J, Arsuaga JM, Arencibia A, Lindo M, Gascón V (2009) Aqueous heavy metals removal by adsorption on amine-functionalized mesoporous silica. J Hazard Mater 163:213–221

Al Hamouz OCS, Estatie MTA (2017) Saleh removal of cadmium ions from wastewater by dithiocarbamate functionalized pyrrole based terpolymers. Sep Purif Technol 177:101–109

Azizi N, Khajeh M, Alipour M (2014) Rapid and selective oxidation of alcohols in deep eutectic solvent. Ind Eng Chem Res 53:15561–15565

Azizi N, Aryanasab F, Saidi MR (2006) Straightforward and highly efficient catalyst-free one-pot synthesis of dithiocarbamates under solvent-free conditions. Org Lett 8:5275–5277

Bai L, Hu H, Fu W, Wan J, Cheng X, Zhuge L, Xiong L, Chen Q (2011) Synthesis of a novel silica-supported dithiocarbamate adsorbent and its properties for the removal of heavy metal ions. J Hazard Mater 195:261–275

Baytak S, Türker AR (2009) Determination of chromium, cadmium, and manganese in water and fish samples after preconcentration using Penicillium digitatum immobilized on pumice stone. Clean–Soil, Air, Water 37:314–318

Baraka A, Hall PJ, Heslop M (2007) Melamine–formaldehyde–NTA chelating gel resin: Synthesis, Characterization, and application for copper (II) ion removal from synthetic wastewater. J Hazard Mater 140:86–94

Biswas FB, Rahman IMM, Nakakubo K, Yunoshita K, Endo M, Nagai K, Mashio AS, Taniguchi T, Nishimura T, Maeda K, Hasegawa H (2021) Selective recovery of silver and palladium from acidic waste solutions using dithiocarbamate-functionalized cellulose. Chem Eng J 407:127225

Chen X, Lam KF, Zhang Q, Pan B, Arruebo M, Yeung KL (2009) Synthesis of highly selective magnetic mesoporous adsorbent. J Phys Chem C 113:9804–9813

Catalfamo P, Arrigo I, Primerano P, Corigliano F (2006) Efficiency of a zeolitized pumice waste as a low-cost heavy metals adsorbent. J Hazard Mater 134:140–143

Dong X, Meng QW, Hu W, Chen R, Ge Q (2022) Forward osmosis membrane developed from the chelation of Fe3+ and carboxylate for trace organic contaminants removal. Chem Eng J 428:131091

Dolatyari L, Yaftian MR, Rostamnia S (2016) Removal of uranium(VI) ions from aqueous solutions using Schiff base functionalized SBA-15 mesoporous silica materials. J Environ Manag 169:8–17

Friberg L, Nordberg GF, Vouk B (1979) Handbook on the toxicology of metals. Elsevier/North-Holland Biomedical Press, Amsterdam

Feng N, Guo X, Liang S (2009) Adsorption study of copper (II) by chemically modified orange peel. J Hazard Mater 30:1286–1292

Fu W, Huang Z (2018) Magnetic dithiocarbamate functionalized reduced graphene oxide for the removal of Cu(II), Cd(II), Pb(II), and Hg(II) ions from aqueous solution: synthesis, adsorption, and regeneration. Chemosphere 209:449–456

Jing XS, Liu FQ, Yang X, Ling PP, Li LJ, Long C, Li A (2009) Adsorption performances and mechanisms of the newly synthesized N,N′-di (carboxymethyl) dithiocarbamate chelating resin toward divalent heavy metal ions from aqueous media. J Hazard Mater 167:589–596

Johnson BB (1990) Effects of pH, temperature, and concentration on the adsorption of cadmium on goethite. Environ Sci Technol 24:112–118

Huang H, Luo Y, Wang H, Zeng G, Li X (2020) Recent advances in dithiocarbamate-based adsorbents for heavy metal removal from wastewater. Sci Total Environ 709:136218

Hong J, Kang L, Shi X, Wei R, Mai X, Pan D, Naik N, Guo Z (2022) Highly efficient removal of trace lead (II) from wastewater by 1,4-dicarboxybenzene modified Fe/Co metal-organic nanosheets. J Mater Sci Technol 98:212–218

Ibrahim Y, Wadi VS, Ouda M, Naddeo V, Banat F, Hasan SW (2022) Highly selective heavy metal ions membranes combining sulfonated polyethersulfone and self-assembled manganese oxide nanosheets on positively functionalized graphene oxide nanosheets. Chem Eng J 428:131267

Iqbal M, Saeed A, Kalim I (2009) Characterization of adsorptive capacity and investigation of mechanism of Cu(II), Ni2+ and Zn2+ adsorption on mango peel waste from constituted metal solution and genuine electroplating effluent. Sep Sci Technol 30:3770–3791

Girginova PI, Daniel-da-Silva AL, Lopes CB, Figueira P, Otero M, Amaral VS, Pereira E, Trindade T (2010) Silica coated magnetite particles for magnetic removal of Hg2+ from water. J Colloid Interface Sci 345:234–240

Goubert-Renaudin S, Gaslain F, Marichal C, Lebeau B, Schneider R, Walcarius A (2009a) Synthesis of dithiocarbamate-functionalized mesoporous silica-based materials: interest of one-step grafting. New J Chem 33:528–537

Goel J, Kadirvelu K, Rajagopal C, Garg VK (2005) Removal of lead (II) by adsorption using treated granular activated carbon: batch and column studies. J Hazard Mater 125:211–220

Gardea-Torresdey JL, Hernandez A, Tiemann KJ, Bibb J, Rodriguez O (1998) Adsorption of toxic metal ions from solution by inactivated cells of Larrea tridentata creosote bush. J Hazard Mater 1:3–8

Goubert-Renaudin S, Gaslain F, Marichal C, Lebeau B, Schneider R, Walcarius A (2009b) Synthesis of dithiocarbamate-functionalized mesoporous silica-based materials: interest of one-step grafting. New J Chem 33:528–537

Kosa SA, Al-Zhrani G, Salam MA (2012) Removal of heavy metals from aqueous solutions by multi-walled carbon nanotubes modified with 8-hydroxyquinoline. Chem Eng 181:159–168

Kim MY, Lee TG (2019) Removal of Pb (II) ions from aqueous solutions using functionalized cryogels. Chemosphere 217:423–429

Lo W, Chua H, Lam KH, Bi SP (1999) A comparative investigation on the biosorption of lead by filamentous fungal biomass. Chemosphere. 39:2723–2736

Li X, Zhang Y, Zhang L, Liu Y (2020) Dithiocarbamate-based adsorbents for heavy metal removal and their applications: a critical review. J Mol Liq 302:112528

Madoni P, Davoli D, Gorbi G, Vescovi L (1996) Toxic effect of heavy metals on the activated sludge protozoan community. Water Res 30:135–142

Moraci N, Calabrò PS (2010) Heavy metals removal and hydraulic performance in zero-valent iron/pumice permeable reactive barriers. J Environ Manage 91:2336–2341

Mahmoud ME (1999) Selective solid-phase extraction of mercury (II) by silica gel-immobilized-dithiocarbamate derivatives. Anal Chim Acta 398:297–304

Mahmoud ME, El-Essawi MM, Fathallah EMI (2004) Characterization of surface modification, thermal stability, and metal selectivity properties of silica gel phases-immobilized dithiocarbamate derivatives. J Liq Chromatogr 27L:1711–1727

Mishra P, Patnaik S, Parida K (2019) An overview of recent progress on noble metal modified magnetic Fe3O4 for photocatalytic pollutant degradation and H2 evolution. Cat Sci Technol 9:916–941

McKittrick MW, Jones CW (2003) Toward single-site functional materials preparation of amine-functionalized surfaces exhibiting site-isolated behavior. Chem Mater 15:1132–1139

Salomons W (1995) Environmental impact of metals derived from mining activities: processes, predictions, prevention. J Geochem Explor 52:5–23

Nakakubo K, Hasegaw H, Ito M, Yamazaki K, Miyaguchi M, Biswas FB, Ikai T, Maeda K (2019) Dithiocarbamate-modified cellulose resins: a novel adsorbent for selective removal of arsenite from aqueous media. J Hazard Mater 380:120816

Oh S, Kang T, Kim H, Moon J, Hong S, Yi J (2007) Preparation of novel ceramic membranes modified by mesoporous silica with 3-aminopropyltriethoxysilane (APTES) and its application to Cu(II) separation in the aqueous phase. J Membr Sci 301:118–125

Pournara AD, Rapti S, Lazarides T, Manos MJ (2021) A dithiocarbamate-functionalized Zr4+ MOF with exceptional capability for sorption of Pb(II) in aqueous media. J Environ Chem Eng 9:105474

Pehlivan E, Altun T, Parlayici Ş (2012) Modified barley straw as a potential biosorbent for removal of copper ions from aqueous solution. Food Chem 15:2229

Raval NP, Shah PU (2019) Dithiocarbamate-based adsorbents for heavy metal removal: a comprehensive review. J Environ Chem Eng 7:103439

Tang C, Brodie P, Brunsting M, Chiu K (2020) Carboxylated cellulose cryogel beads via a one-step ester crosslinking of maleic anhydride for copper ions removal. Carbohydr Polym 242:116397

Sari A, Tuzen M (2019) Dithiocarbamate-based adsorbents for heavy metal removal: a critical review. J Hazard Mater 368:482–504

Sari A, Tuzen M (2017) Dithiocarbamate-based adsorbents for heavy metal removal from water: a review. J Hazard Mater 344:179–200

Siegel H, Martin RB (1994) The colorless "Chameleon" or the peculiar properties of $Zn^{2+}$ in complexes in solution. Quantification of equilibria involving a change of the coordination number of the metal ion. Chem Soc Rev 23:83–91

Seyyed Shahabi S, Azizi N, Vatanpour V (2019) Synthesis and characterization of novel g-C3N4 modified thin-film nanocomposite reverse osmosis membranes to enhance desalination performance and fouling resistance. Sep Purif Technol 215:430–440

Shama SA, Gad MA (2010) Removal of heavy metals (Fe3+, Cu(II), Zn2+, Pb(II), Cr3+, and Cd(II)) from aqueous solutions by using hebba clay and activated carbon. Port Electrochim Acta 28:231–239

Shuklov IA, Dubrovina NV, Boerner A (2007) Fluorinated alcohols as solvents, cosolvents and additives in homogeneous catalysis. Synthesis 19:2925–2943

Waseem M, Mustafa S, Naeem A, Koper GJM, Shah KH (2011) Cd(II) sorption characteristics or iron-coated silica. Desalination 277:221–226

Wang L, Wang K, Huang R, Qin Z, Su Y, Tong S (2020) Hierarchically flower-like WS2 microcrystals for capture and recovery of Au (III), Ag (I), and Pd (II). Chemosphere 252:126578

Wang Y, Gao B, Yue Q, Li Q (2018) Recent advances in dithiocarbamate-functionalized adsorbents for heavy metal removal from water. Chem Eng J 333:622–635

Ho Y, Porter J, McKay G (2002) Equilibrium isotherm studies for the sorption of divalent metal ions onto peat: copper, nickel and lead single component systems. Water Air Soil Pollut 141:1–33

Yaqoob SB, Adnan R, Rameez Khan RM, Gold RM (2020) silver, and palladium nanoparticles: a chemical tool for biomedical applications. Front Chem 8:1–15

Yu H, Zhu Y, Hui A, Wang A (2022) Novel eco-friendly spherical porous adsorbent fabricated from pickering middle internal phase emulsions for removal of Pb(II) and Cd (II). J Environ Sci 112:320–330

Yazdani F, Fattahi B, Azizi N (2016) Synthesis of functionalized magnetite nanoparticles to use as liver targeting MRI contrast agent. J Magn Magn Mater 406:207–211

Zhang J, Zheng Y, Chen C, Zhu X, Wang A (2020) Recent advances in dithiocarbamate-based adsorbents for the removal of heavy metal ions: synthesis, characterization, and applications. Chem Eng J 397:125390

Zhang Y, Zhang L, Zhang M, Chen J, Zhang Z, Zhu X (2019) Dithiocarbamate-based adsorbents for heavy metal ions removal: a review. J Hazard Mater 369:521–533

Zhang L, Zhang Y, Sun X, Zhang M, Yang F (2021) Dithiocarbamate-based adsorbents for heavy metal removal: challenges and future perspectives. Chemosphere 262:127938